ORIGINAL ARTICLE

Targeting of 4-1BB by monoclonal antibody PF-05082566 enhances T-cell function and promotes anti-tumor activity

Timothy S. Fisher · Cris Kamperschroer · Theodore Oliphant · Victoria A. Love ·
Paul D. Lira · Regis Doyonnas · Simon Bergqvist · Sangita M. Baxi ·
Allison Rohner · Amy C. Shen · Chunli Huang · Sharon A. Sokolowski ·
Leslie L. Sharp

Abstract 4-1BB (CD137, TNFRSF9) is a costimulatory receptor expressed on several subsets of activated immune cells. Numerous studies of mouse and human T cells indicate that 4-1BB promotes cellular proliferation, survival, and cytokine production. 4-1BB agonist mAbs have demonstrated efficacy in prophylactic and therapeutic settings in both monotherapy and combination therapy tumor models and have established durable anti-tumor protective T-cell memory responses. PF-05082566 is a fully human IgG2 that binds to the extracellular domain of human 4-1BB with high affinity and specificity. In preclinical studies, this agonist antibody demonstrated its ability to activate NF-κB and induce downstream cytokine production, promote leukocyte proliferation, and inhibit tumor growth in a human PBMC xenograft tumor model. The mechanism of action and robust anti-tumor efficacy of PF-05082566 support its clinical development for the treatment of a broad spectrum of human malignancies.

Keywords CD137 · TNFRSF9 · Agonist monoclonal antibody · Immunotherapy · T cell · Cancer

T. S. Fisher · V. A. Love · P. D. Lira · S. Bergqvist ·
S. M. Baxi · A. Rohner · L. L. Sharp (✉)
Oncology Research Unit, Pfizer Inc., 10724 Science Center
Drive, San Diego, CA 92121, USA
e-mail: lesliesharp1@gmail.com

C. Kamperschroer
Immunotoxicology Center of Emphasis, Drug Safety Research
and Development, Pfizer Inc., Groton, CT, USA

T. Oliphant
Protein Therapeutics Center of Emphasis, Pfizer Inc.,
700 Chesterfield Parkway West, Chesterfield,
MO 63017, USA

R. Doyonnas
Genetically Engineered Models Center of Emphasis, Pfizer Inc.,
Eastern Point Road, Groton, CT 06340, USA

A. C. Shen · C. Huang · S. A. Sokolowski
Biomarkers Flow Cytometry Core Facility, Drug Safety
Research and Development, Pfizer Inc.,
Eastern Point Road, Groton, CT 06340, USA

Introduction

4-1BB (CD137, TNFRSF9), first identified as an inducible co-stimulatory receptor expressed on activated T cells, is a membrane-spanning glycoprotein of the tumor necrosis factor (TNF) receptor superfamily (TNFRSF). Current understanding of 4-1BB indicates that expression is generally activation dependent and encompasses a broad subset of immune cells including activated T cells, activated natural killer (NK) and natural killer T (NKT) cells, regulatory T cells, dendritic cells (DC) including follicular DC, stimulated mast cells, differentiating myeloid cells, monocytes, neutrophils, and eosinophils [1]. 4-1BB expression has also been demonstrated on tumor vasculature [2, 3] and atherosclerotic endothelium [4]. The ligand that stimulates 4-1BB (4-1BBL) is expressed on activated antigen-presenting cells (APCs), myeloid progenitor cells, and hematopoietic stem cells [1].

4-1BB is undetectable on the surface of naive T cells. Following in vivo stimulation with antigen or T-cell mitogens, 4-1BB expression peaks at 12–24 h post stimulation, is maintained for an additional 24–48 h, and declines by 72 h [5]. 4-1BB exists in the cytoplasmic membrane of activated T cells as both monomers and dimers [6]. Based

on homology to other members of the TNFRSF, ligand binding is expected to induce receptor trimerization resulting in activation [7]. Some members of the TNFRSF can exist in a soluble form following cleavage of the extracellular domain from the cell surface. Soluble 4-1BB and soluble 4-1BBL have been detected in the serum of some patients with autoimmune diseases and cancers [8–10].

Upon 4-1BB activation, TRAF1 and TRAF2, pro-survival members of the TNFR-associated factor (TRAF) family are recruited to the 4-1BB cytoplasmic tail resulting in downstream activation of NF-κB and the mitogen-activated protein (MAP) kinase cascade including ERK, JNK, and p38 MAP kinases. NF-κB activation leads to upregulation of Bfl-1 and Bcl-XL, pro-survival members of the Bcl-2 family. The pro-apoptotic protein Bim is downregulated in a TRAF1- and ERK-dependent manner [11]. Together, these effects contribute to enhanced survival.

Numerous studies of mouse and human T cells indicate that 4-1BB promotes cellular proliferation, survival, and cytokine production. 4-1BB agonist mAbs have been shown to increase co-stimulatory molecule expression and markedly enhance cytolytic T lymphocyte responses [12]. Agonist 4-1BB mAbs as monotherapy or in combination with other therapies have provided evidence of anti-tumor benefit in prophylactic and therapeutic settings [13]. Stimulation of 4-1BB has been shown to result in durable anti-tumor protective T-cell memory responses [14]. More recently, 4-1BB agonist mAbs have been shown to increase expression of the cellular adhesion molecules ICAM-1, VCAM-1, and E-selectin on tumor vasculature resulting in increased T-cell migration into tumor lesions [15]. 4-1BB agonists have been demonstrated to inhibit autoimmune reactions in a variety of autoimmunity models [16]. However, high doses of 4-1BB agonist mAbs in naive and tumor-bearing mice have been reported to induce T-cell infiltration to the liver and elevations of aspartate aminotransferase (AST) and alanine aminotransferase (ALT) consistent with liver inflammation [17, 18]. Initial clinical studies into the human therapeutic use of 4-1BB agonist mAbs have also demonstrated elevation of liver enzymes and increased incidence of hepatitis [19, 20]. Therefore, while 4-1BB agonist mAbs hold promise for clinical use, care must be taken to assess alterations in immune system and organ function to achieve dosing regimens that maximize therapeutic potential while minimizing risks for toxicity.

The present study describes the identification and characterization of PF-05082566, a potent mAb that selectively agonizes human 4-1BB. PF-05082566 potently activates NF-κB resulting in increased proliferation and cytokine production of human T cells. Anti-tumor efficacy of PF-05082566 was demonstrated in huPBL-SCID xenograft models. PF-05082566 is currently in clinical development for the treatment of advanced solid tumors and B-cell malignancies.

Materials and methods

Animals

All animal experiments were carried out in strict compliance with Institutional Animal Care and Use Committee (IACUC) guidelines and in accordance with the "Guide for the Care and Use of Laboratory Animals" (1996) by the Institute of Laboratory Animals Research Commission on Life Sciences (ILARCLS, National Research Council, Washington, DC). All handling and procedures were documented on an IACUC approved Animal Use Protocol (AUP). NOD.Cg-Prkdc^{scid} Il2rg^{tmlWjl}/SzJ (NSG) mice were purchased from The Jackson Laboratory. CB17.Cg-Prkdc^{scid} Lyst^{bg}/Crl (SCID-bg) mice were purchased from Charles River Laboratories. For all studies involving immune-compromised mice, animals were housed in barrier rooms under pathogen-free conditions. Studies with non-human primates were performed using cynomolgus macaques of Mauritian origin obtained through Charles River Laboratories.

Antibodies

The following antibodies were made at Pfizer: PF-0508 2566 (a fully human IgG2 mAb), negative control mAbs keyhole limpet hemocyanin (KLH)-IgG2 and MOR3207-IgG2 (a fully human IgG2 mAb generated with Fab region specific for lysozyme).

Generation of fully human anti-4-1BB antibodies

PF-05082566 was derived from a Fab which was selected from the MorphoSys AG HuCAL GOLD phage display library on the basis of binding to 4-1BB during two alternating rounds of panning on human 4-1BB-expressing 293T cells and recombinant human 4-1BB-IgG1Fc fusion protein followed by affinity maturation using MorphoSys AG RapMAT technology. One non-germline framework mutation in the heavy chain and six non-germline framework mutations in the light chain were reverted to germline sequence. Expression and purification techniques may be found in Supplementary Methods.

4-1BB binding assays and affinity determination

Antibody binding and affinity for 4-1BB extracellular domain (ECD) were measured by fluorescence-activated cell sorting (FACS), enzyme-linked immunosorbent assay

(ELISA), and surface plasmon resonance (SPR) biosensor assay. Assessment of interference between 4-1BB and 4-1BBL was measured using ELISA. Details of techniques may be found in Supplementary Methods.

Cells

300.19 and 293T cells were maintained in DMEM High Glucose 1× (GIBCO-Invitrogen) containing 10% fetal bovine serum, 1× Glutamax (GIBCO-Invitrogen), 1× MEM nonessential amino acids, 50 U/ml penicillin, 50 μg/ml streptomycin, and 55 μM 2-mercaptoethanol. Cells were transduced with pCL-10A1 (Imgenex) pseudotyped pMSCV_puro (Clontech) retrovirus and selected with puromycin selection to generate human 4-1BB-, cyno 4-1BB-, dog 4-1BB-, human OX-40-, and human CD40-expressing cell pools.

PBMC isolation

Human whole blood was collected from healthy volunteer donors and PBMC isolated using Accuspin tubes (Sigma) following manufacturer recommendation. Whole blood from cynomolgus (cyno) monkey was collected in CPT vacutainer tubes (BD Bioscience) and PBMC isolated following manufacturer recommendations. Whole blood from rat or dog was collected in heparinized vacutainer tubes. PBMCs were isolated using Lympholyte-Mammal (Cedarlane Laboratories) following manufacturer instructions.

In vitro NF-κB activation assay

293T cells stably transduced with lentivirus to introduce an NF-κB-luciferase reporter construct were transduced with human 4-1BB retrovirus. 293T cells stably transduced to express cyno 4-1BB were transiently transfected with an NF-κB-luciferase reporter plasmid along with a renilla luciferase-expressing control plasmid, pRL-CMV (Promega). For all samples, cells were harvested and stimulated for 5 h with varied concentrations of PF-05082566 or human IgG2 control antibody using 2.5× concentration of goat anti-human IgG-Fc F(ab′)2 (Thermo Scientific) to cross-link the human antibody. Luciferase activity was evaluated with Bright Glo luciferase assay or Dual Glo luciferase (Promega) assay for human 4-1BB and cyno 4-1BB assays, respectively.

In vitro human T-cell IL-2 release assay

Human T cells were isolated via negative selection from freshly isolated PBMC using T-cell purification columns (R&D Systems) following manufacturer protocol. One hundred thousand T cells/well were stimulated with 10 μg/ml anti-CD3 clone UCHT-1 (Biolegend) in the presence of

varying concentrations of PF-05082566 or control human IgG2 in RPMI (GIBCO-Invitrogen) containing 10% FBS, 1× MEM nonessential amino acids, HEPES, 50 U/ml penicillin, and 50 μg/ml streptomycin. Human IL-2 production was assayed via ELISA (R&D Systems) of culture supernatant at 72 h post stimulation.

In vitro antigen-specific T-cell expansion assay

Primary human PBMCs were collected from human leukocyte antigen (HLA)-A2+ donors that had received an influenza vaccine within the past year but not less than 60 days prior to collection. PBMCs were cultured at five hundred thousand cells/well in a 24-well plate for 8 days in the presence of a peptide corresponding to influenza matrix peptide 58–66 (GILGFVFTL) (ProImmune) and the indicated concentration of PF-05082566 or a human IgG2 control antibody. Cells were harvested and stained with antibodies to CD3, CD8, and a pentameric major histocompatibility complex (MHC) HLA-A2-GILGFVFTL peptide reagent (ProImmune) and assessed via FACS.

In vitro phospho-NF-κB assay

Purified human or cynomolgus monkey T cells (2 million/well) were seeded onto 24-well plates coated with 2 μg/ml anti-CD3 clone UCHT1 or clone SP34 (BD Pharmingen), respectively, and cultured for 48 h. Activated cells were harvested and re-stimulated for 10 min on 24-well plates coated with 2 μg/ml of anti-CD3 alone or with the addition of PF-05082566 that had previously been cross-linked via the addition of goat anti-human IgG-Fc F(ab′)2. Cells were fixed and permeabilized prior to staining with anti-human 4-1BB and anti-phospho-NF-κB p65 antibodies and analyzed via FACS.

huPBL-NSG in vivo lymphocyte expansion model

Ten million freshly isolated human PBMCs were adoptively transferred via intraperitoneal injection into NSG host mice. Nine days post PBMC injections, animals were administered a single dose of the indicated concentration of PF-05082566 or isotype control antibody via intraperitoneal injection. Upon study termination (day 28 post PBMC engraftment, day 19 post antibody injection) PBMCs were stained with antibodies to human and mouse CD45 and Ki-67 and assessed via FACS.

Evaluation of proliferation in cynomolgus monkey

Cynomolgus monkeys were given intravenous injections of PF-05082566 at the indicated dose. Blood was collected into tubes containing K_2EDTA prior to the antibody dose

(pre-dose) and on the indicated study days relative to administration of PF-05082566 (given on Study Day 1). Peripheral blood cells were stained with antibodies against CD3, CD4, CD8, CD16, CD28, CD95, followed by intracellular staining for Ki-67, and then erythrocytes were lysed using FACSLyse solution (Becton–Dickinson). Cells were analyzed using a Canto II flow cytometer (Becton–Dickinson) with DIVA software version 6.1.1 (Becton–Dickinson). CD8+ central memory T cells were identified as CD3+, CD8+, CD28+, and CD95+; CD8+ effector memory T cells were identified as CD3+, CD8+, CD28−, and CD95+; and NK cells were identified as CD3−CD8+CD16+. Proliferating cells were identified as Ki-67+.

huPBL-SCID-Bg in vivo anti-tumor efficacy model

PC3, LoVo, and WM-266 tumor cell lines were obtained from ATCC and cultured according to guidelines provided. One and a half million freshly isolated PBMCs were mixed with three million tumor cells and implanted on the flank of SCID-bg mice. Animals were randomized based on tumor size on Day 7 post implantation and given a single dose of the indicated concentrations of PF-05082566 or vehicle control. Tumors were measured two to three times per week until study termination. Tumor Volume is calculated (length $\times$ (width $\times$ width) $\times$ 0.5) = volume in mm^3.

Results

4-1BB-binding affinity and selectivity of PF-05082566

PF-05082566 showed reversible binding to recombinant human 4-1BB by SPR analysis. The observed equilibrium dissociation constant (K_D) for 4-1BB ECD was 8.7 ± 1.0 nM. In similar studies using isolated Fab from PF-05082566, a K_D of 69 ± 3 nM was observed. Binding of PF-05082566 to recombinant human 4-1BB ECD was also determined via ELISA binding assay, with an observed EC_{50} of 0.124 ± 0.041 nM. PF-05082566 bound competitively with recombinant human 4-1BB ligand (4-1BBL) to recombinant human 4-1BB, with an observed IC_{50} of 0.20 ± 0.003 nM. Binding of PF-05082566 to cell membrane bound 4-1BB was measured using flow cytometry (FACS) with a mouse pre-B-cell line (300.19) retrovirally transduced to express human 4-1BB or with phytohemagglutinin (PHA)-stimulated primary human PBMC (Fig. 1a, c). The mean EC_{50} of binding to transduced cells was determined to be 1.8 nM, whereas the mean EC_{50} of binding to activated PBMC was 48.9 nM.

Human 4-1BB shares approximately 50% amino acid identity with rodent 4-1BB, whereas, cynomolgus monkey 4-1BB is highly homologous to that of human 4-1BB with

95% identity in amino acid sequence [21]. By SPR, the observed K_D for the PF-05082566 Fab binding to recombinant cyno 4-1BB was 96 ± 1 nM. Solution binding studies by isothermal titration calorimetry (ITC) confirmed an expected binding stoichiometry of 2:1 (2 X 4-1BB per PF-05082566). By ELISA an EC_{50} of 0.198 ± 0.027 nM for binding of PF-05082566 to recombinant cyno 4-1BB was observed. Binding of PF-05082566 to cyno 4-1BB was also measured with retrovirally transduced 300.19 cells and PHA-stimulated PBMC. The mean EC_{50} for binding to transduced cells was 4.2 nM compared with 149 ± 68 nM for activated cyno PBMC (Fig. 1b, d). No binding to dog or rat 4-1BB was detected by FACS analysis of PHA-stimulated PBMC at concentrations of PF-05082566 up to 100 nM. Further, PF-05082566 did not bind to 300.19 cells transduced to express dog 4-1BB at concentrations up to 1,000 nM. In conclusion, PF-05082566 only recognizes human and cyno 4-1BB and is not selective for dog or rat 4-1BB. Kinetic studies directly comparing the binding of the PF-05082566 Fab to human and cyno 4-1BB indicated less than a 1.5-fold higher K_D for human compared with cyno 4-1BB. By ELISA and FACS analysis, an average decrease in affinity of 2.6-fold for cyno compared with human 4-1BB was observed.

The selectivity of PF-05082566 parent mAb for 4-1BB was assessed against other members of the TNFR superfamily via FACS. 300.19 cells transduced to express the ECD or full-length protein of related receptors, CD40 (TNFRSF5) and OX-40 (CD134, TNFRSF4), were stained. No significant binding was observed at concentrations up to 1000 nM to these receptors, demonstrating >100-fold selective binding for 4-1BB versus related family members (data not shown).

PF-05082566 enhances NF-κB signaling in vitro

The functional activity of PF-05082566 was demonstrated on both 4-1BB transduced cells and on primary T cells. In these assays, PF-05082566 demonstrated agonist activity when added to cells in the presence of a F(ab')2 goat anti-human IgG secondary agent (cross-linked), or when immobilized via binding to tissue culture plastic (plate-bound).

PF-05082566 was assessed for agonist activity using 293T cells transduced with full length human or cynomolgus 4-1BB and an NF-κB luciferase reporter. In this assay, PF-05082566 enhanced NF-κB signaling through human 4-1BB with a mean EC50 of 0.15 ± 0.04 nM, and cyno 4-1BB with a mean EC50 of 0.4 ± 0.04 nM. Representative concentration–response curves for the induction of luciferase by PF-05082566 are shown in Fig. 2a, b. Similarly, cross-linked PF-05082566 rapidly induced NF-κB phosphorylation upon re-stimulation of CD3-stimulated primary
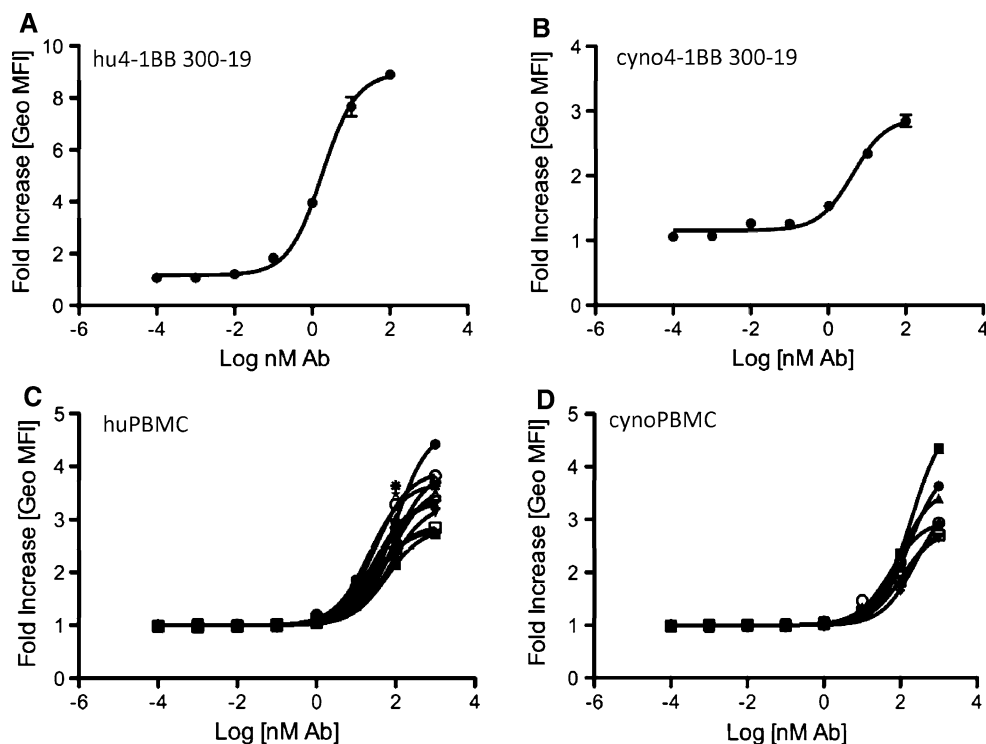
Fig. 1 Saturation binding of PF-05082566 to human and cynomolgus monkey 4-1BB. Dose-dependent binding of AlexaFluor647-labeled PF-05082566 to **a** 300-19 cells transduced to express human 4-1BB, **b** 300-19 cells transduced to express cynomolgus monkey 4-1BB, **c** 72-h PHA-stimulated primary human PBMC, and **d** 72-h PHA-stimulated primary cynomolgus monkey PBMC. The data are expressed as fold increase in geometric mean fluorescence intensity (Geo MFI) of cells stained with PF-05082566 relative to cells stained with the corresponding concentration of human IgG2 isotype control as measured by FACS. **a**, **b** display data from representative experiments with samples stained in duplicate. *Error bars* represent SEM. **c**, **d** represent data of binding to 72-h PHA-stimulated CD3-positive primary PBMC. Each line represents the staining result of cells isolated from individual donors. Representative examples of flow cytometry data are demonstrated in Supplementary Figure 1 for 300-19 cells and Supplementary Figure 2 for PBMC

human and cynomolgus T cells (Fig. 2c, d) as measured by intracellular staining of phospho-NF-κB p65. Changes in NF-kB phosphorylation were statistically significant in some but not all donors tested.

PF-05082566 induces human T cell cytokine release and proliferation in vitro

PF-05082566 also enhances anti-CD3-mediated interleukin 2 (IL-2) production by isolated human primary T cells. Although the signal to noise ratio was low in some assays due to the induction of IL-2 by anti-CD3 alone, PF-05082566 enhanced IL-2 production when anti-CD3 and PF-05082566 were simultaneously bound in the assay well. No activity was observed for PF-05082566 on freshly isolated T cells in the absence of anti-CD3 (data not shown). The magnitude of IL-2 augmentation by PF-05082566 ranged from 2- to 20-fold versus anti-CD3 plus IgG2 isotype control depending on the donor and the amount of IL-2 generated by anti-CD3 plus control antibody. The average EC_{50} calculated from experiments using an 8-point concentration response curve was

22.6 $\pm$ 7.63 nM (Fig. 3a). IL-2 production in response to anti-CD3 stimulation has resulted in less IL-2 being produced at higher concentrations of PF-05082566. The reason for this bell-shaped curve is unclear but could be due to inefficient anti-CD3-mediated activation due binding hindrance resulting from the large amount of PF-05082566 present on the plate surface. Alternatively, it could potentially relate to utilization of IL-2 in culture by CD3-activated cells.

PF-05082566 was also shown to enhance antigen-specific T-cell proliferation. PBMCs derived from HLA-A2+ donors previously vaccinated for influenza were cultured with a peptide from the influenza M protein. Following culture, samples that included PF-05082566 had an increased percentage of antigen-specific CD8+ T cells as revealed by peptide-specific MHC pentamer staining when compared with samples that had been treated with a control antibody. The magnitude of increased antigen-specific T cells induced by PF-05082566 ranged from two- to eight-fold versus peptide plus IgG2 isotype control depending on the donor and the amount of antigen-specific T cells generated by peptide plus control antibody (Fig. 3b).
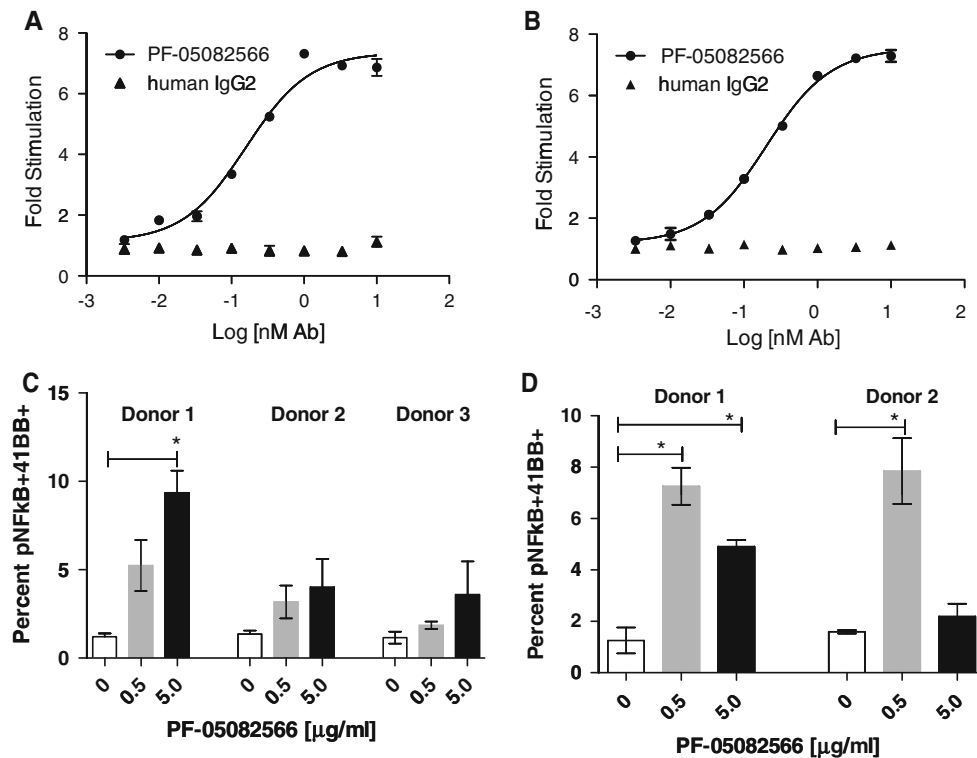
Fig. 2 PF-05082566 induces NF-κB pathway activation through both human and cynomolgus monkey 4-1BB. Dose-dependent activation of an NF-κB luciferase reporter in a 293T-cells-expressing human 4-1BB or b 293T-cells-expressing cynomolgus monkey 4-1BB. The data are representative of three separate experiments and shows fold increase in luciferase activity over unstimulated control cells by goat anti-huIgG Fc-specific F(ab')2 cross-linking antibody plus PF-05082566 (black circles) or cross-linked human IgG2 isotype control (black triangles). Additionally, PF-05082566 treatment induces phospho-NF-κB p65 in anti-CD3-stimulated primary c human and d cynomolgus monkey CD3+ cells. The graphs demonstrate percentage of phospho-NF-κB p65+, 4-1BB+ T cells as measured by FACS. Cells were stimulated with CD3 alone (white bars), CD3 plus cross-linked 0.5 μg/ml PF-05082566 (gray bars), or CD3 plus cross-linked 5 μg/ml PF-05082566 (black bars). Significance relative to the control group was determined via two-tailed Student's t test (*$p < 0.05$)
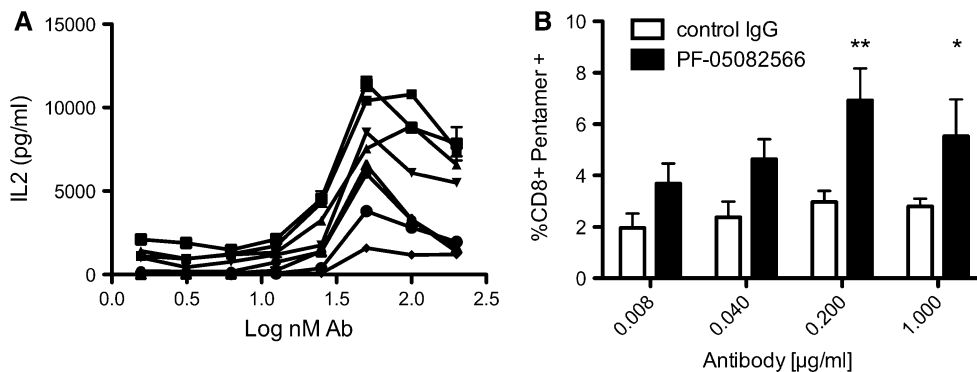

Fig. 3 PF-05082566 enhances IL-2 production by primary human T cells and expansion of antigen-specific CD8+ T cells in vitro. a Dose-dependent enhancement of IL-2 production as measured by ELISA from purified T cells stimulated with plate bound CD3 plus increasing concentrations of plate bound PF-05082566. Each line represents stimulation of purified T cells from one of seven individual donors tested in duplicate. b PBMC isolated from four separate HLA-A2+ donors whom had received an influenza vaccine within the prior season were stimulated in vitro with influenza matrix peptide (58–66, GILGFVFTL) for 8 days in the presence of either huIgG2 control antibody (white bars) or PF-05082566 (black bars). The data are represented as the percent viable CD8+, MHC HLA-A2-GIL-GFVFTL pentamer+ cells as measured by FACS. Significance was determined via 2-way ANOVA comparison with the control IgG2-treated group (**$p < 0.01$, *$p < 0.05$). Results are representative of two separate experiments using four different donors

In vitro studies using primary lymphocytes derived from healthy human and cynomolgus donors showed a large variation of response in both proximal signaling events and effector function. This likely represents the response range from a genetically and environmentally heterogeneous populations.

PF-05082566 induces human lymphocyte proliferation in vivo

The lack of PF-05082566 cross-reactivity with murine 4-1BB required the development of novel small animal models for the in vivo functional assessment of PF-05082566. Mice with the NOD genetic background carrying the severe combined immunodeficient (SCID) mutation and deficiency in the IL-2 receptor common gamma chain (commonly termed NSG) are able to support the engraftment of large numbers of human peripheral blood leukocytes (huPBL). Following engraftment, T cells rapidly acquire an activated phenotype and can maintain engraftment for 30 days before the onset of graft versus host disease [22]. This huPBL-NSG model represents a small animal model in which to assess the functional effect of in vivo systemic administration of PF-05082566 on human immune cells. PF-05082566 was able to enhance expansion of human leukocytes in a dose-dependent manner as evidenced by an increase in the proportion of human CD45+ cells in the peripheral blood of engrafted mice. Similarly, there was a dose-dependent increase in the proportion of human leukocytes expressing the proliferation marker Ki-67 (Fig. 4).
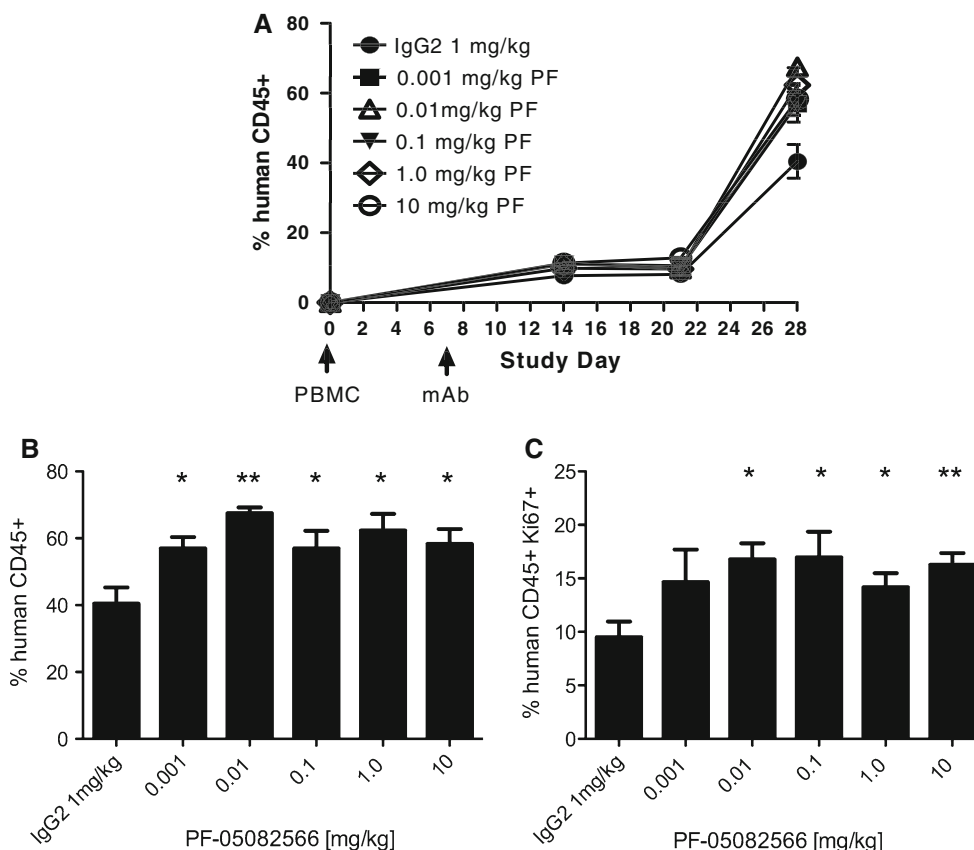

Fig. 4 PF-05082566 induces expansion of human CD45+ PBMC in vivo. Engraftment of human PBMC adoptively transferred via intraperitoneal injection to NSG host mice was analyzed by FACS for human CD45 and Ki-67 staining 28 days following injection. On day 7 following PBMC injection, mice were treated with a single injection of human IgG2 isotype control or the indicated concentration of PF-05082566. **a** Mean percentage of human CD45+ lymphocytes assessed at several time points over the course of the study **b** percentage of human CD45+ lymphocytes at Study Day 28, 21 days following mAb injection and **c** percentage of human CD45+ Ki-67+ present in the whole blood samples of each treatment group at Study Day 28, 21 days following mAb injection. Data are representative of $n = 7$ mice per group and significance relative to the control group on the final day of the study was determined via two-tailed Student's t test ($*p < 0.05$, $**p < 0.005$)

PF-05082566 induces cynomolgus monkey lymphocyte proliferation in vivo

To assess proliferation among memory T cells, blood samples were isolated from cynomolgus monkeys at several time points following single or multiple intravenous doses of PF-05082566. Using flow cytometry, memory subsets of CD4 T cells and CD8 T cells were identified using CD95 and CD28 as markers of central memory (CD95+ CD28+) and effector memory (CD95+ CD28−) subsets in macaques [23]. Ki-67 was analyzed as a proliferation marker.

In a multiple dose study, which assessed weekly doses of PF-05082566 at 0.3, 5, and 100 mg/kg, there were large increases on study day 13 in the numbers of proliferating peripheral blood CD8+ central memory T cells (CD8+ T_{CM}) in individual animals in all dose groups, and the 5 and 100 mg/kg groups were significantly increased relative to the vehicle control group (Fig. 5a, b). Parallel increases were observed in the numbers of total CD8+ T_{CM} in individuals of all groups except females at the 0.3 mg/kg dose level. Similar trends were observed with CD8+ effector memory T cells (CD8+ T_{EM}) on study day 13, but the effects were generally of lower magnitudes/frequencies than those on CD8+ T_{CM}, and increases in Ki-67+ CD8+ T_{EM} in treated groups were statistically significant only at 5 mg/kg (Fig. 5b). Numbers of all proliferating CD8 memory T-cell subsets returned to baseline by study day 43. Among CD4 T cells, little or no increases were observed in Ki-67+ cells in central or effector memory subsets (data not shown). Proliferation among other T-cell subsets or among NK cells was not examined in the multiple dose study. It should be noted that the presence of anti-drug antibodies was detected beginning at approximately 14 days following the first dose of PF-05082566 (data not shown). In the multiple dose study, PF-05082566 exposure was decreased to undetectable levels at administrations given on day 36 or greater.

PF-05082566 doses of 0.001, 0.005, 0.05, 0.3, 1 and 10 mg/kg were tested as a single dose over a 28 day period. Within CD8+ T_{CM} a 1.5 fold or greater increase in the number of proliferating (Ki-67+) cells was observed during the first 7 days of the study and was noted in at least one animal in groups treated with 1 mg/kg or greater (Fig. 5c). Increases in proliferating Ki-67+ NK (CD3− CD8+ CD16+) cells were also noted at 0.005 mg/kg (one of two animals), 0.05 and 0.3 mg/kg (two of two animals studied per dose level), but NK cell proliferation was not evaluated at doses higher than 0.3 mg/kg (data not shown). The magnitude of the increases in NK cell proliferation was not dependent on the PF-05082566 dose. The effect of PF-05082566 on other T-cell subsets or on other functional endpoints besides proliferation of T cells and NK cells has not been tested. Overall, the results from cynomolgus macaques show that PF-05082566 induces proliferation of both memory CD8 T cells and NK cells.

Anti-tumor efficacy of PF-05082566

The lack of rodent cross-reactivity of PF-05082566 also prevented the use of standard murine syngeneic or human xenograft tumor models for the assessment of anti-tumor efficacy. Immunodeficient mice have also been demonstrated to support a limited short-term engraftment of human peripheral blood leukocytes (huPBL) [24]. Anti-tumor immune responses have been demonstrated in SCID mice in which lymphocytes and tumor cells were co-engrafted [25]. Therefore, we generated a huPBL-SCID-Bg xenogenic tumor model in which we evaluated the ability of PF-05082566 to modulate the immune response to human tumors. Tumor cell lines were mixed with primary human PBMCs from an allogeneic healthy volunteer donor prior to injection. None of the tumor lines expressed 4-1BB. Once tumors were established at a size of 50 mm³ (generally 5–8 days post injection) animals were treated with PF-05082566. An example growth curve demonstrating the inhibition of tumor growth response to a prostate carcinoma (PC3) is shown in Fig. 6. Tumor cell lines representing melanoma and colon tumor types were also tested in this in vivo model with similar results (Supplemental Figure 3). In general, tumor growth inhibition (TGI) ranged from 40 to 60% relative to control. Efficacy in this model was dependent on the presence of human PBMCs as mice that received injections of tumor cells without co-injection of human PBMCs did not have reduced tumor growth in the presence of PF-05082566 (data not shown).

Discussion

Enhancing anti-tumor immune responses represents a powerful approach for cancer treatment with the potential to provide long-term anti-tumor immunity and to decrease the rate of recurrence. The US Food and Drug Administration approvals of sipuleucel-T (Provenge, Dendreon), a whole cell vaccine for the treatment of advanced prostate cancer and ipilumimab (Yervoy, Bristol-Myers Squibb), a CTLA-4 antagonist mAb for the treatment of unresectable or metastatic melanoma, have demonstrated that modulation of the immune response using a single therapeutic agent has the potential for significant and long-lasting clinical efficacy. Low overall response rates and potential for significant autoimmune toxicities with ipilimumab suggest that further optimization of clinical treatment regimens may benefit a broader patient population [26].
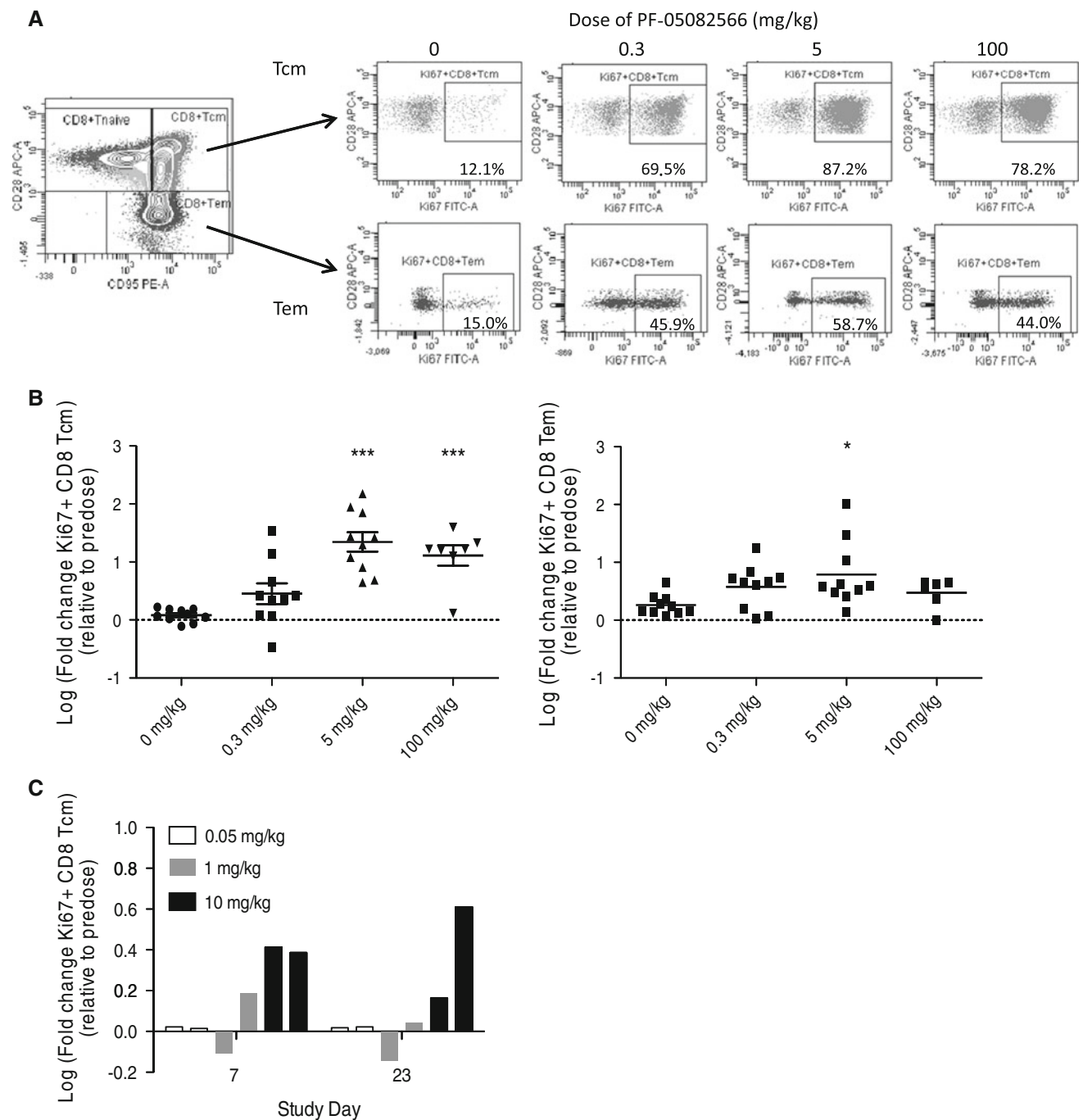
Fig. 5 Intravenous administration of PF-05082566 to cynomolgus monkeys induces proliferation of CD8+ memory T cells. **a, b** Multiple dose administration. Cynomolgus monkeys were injected intravenously with the indicated doses of PF-05082566 on days 1 and 8 of the study ($n = 10$ animals per group). On day 13, blood was collected, and cells were analyzed by flow cytometry. **a** The far *left* plot shows the gating strategy for identifying CD8+ T_{CM} (CD95+ CD28+) and CD8+ T_{EM} (CD95+ CD28−). The remainder of the plots shows representative staining for Ki-67 versus CD28 for CD8+ T_{CM} (*top row*) and CD8+ T_{EM} (*bottom row*) at the indicated dose levels. **b** Multiple dose administration of the indicated dose levels of PF-05082566 on day 1 and day 8 demonstrates significant increases in Ki-67+ CD8+ T_{CM} cells (graph on *left*) and Ki-67+ CD8+ T_{EM} (graph on *right*) as measured on study day 13. **c** Single dose administration of 0.05 mg/kg (*white bars*), 1 mg/kg (*gray bars*), or 10 mg/kg (*black bars*) PF-05082566 to 2 individual animals per group demonstrates increases in Ki-67+ CD8+ T_{CM} cells measured by FACS on study days 7 and 23 post dosing. For both **b** and **c**, fold changes were calculated relative to baseline pre-study samples collected prior to the start of dosing. Statistical significance was calculated using 1-way ANOVA with Dunnett's Multiple Comparison test (*$p < 0.05$, ***$p < 0.001$)
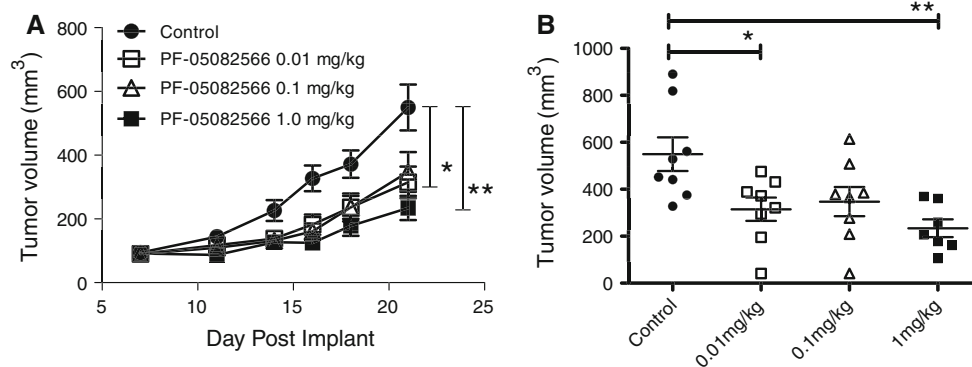
Fig. 6 PF-05082566 inhibits the growth of PC3 prostate carcinoma in vivo. **a** Mean tumor volume at time points following subcutaneous administration of 3 million PC3 prostate carcinoma cells plus 1.5 million human PBMC in the right flank of SCID Bg mice ($n = 8$ animals/group). **b** The volume of each individual tumor on the final study day (day 21). Statistical significance was determined using 1-way ANOVA with Tukey's post-test (*$p < 0.05$, **$p < 0.005$). Data are representative of three independent experiments

Non-clinical data suggest that combinations of immunotherapy agents with certain chemotherapeutics, targeted agents or other immunotherapies have the potential to increase efficacy while minimizing toxicity; however, optimal strategies are yet to be established [27].

The National Cancer Institute immunotherapy agent workshop has identified 4-1BB as an agent with high immunotherapeutic potential with the possibility for broad use in multiple regimens [28]. This potential is supported by a significant body of non-clinical data in which activation of 4-1BB has resulted in anti-tumor efficacy as monotherapy or in combination [13, 29, 30]. Further, T cells modified to express chimeric antigen receptors (CAR) including CD3ζ and 4-1BB signaling domains demonstrated enhanced proliferation and cytokine release in vitro and efficacy in preclinical models of hematologic and solid malignancies [31–34]. Chronic lymphocytic leukemia (CLL) patients treated with autologous CAR T cells targeting CD19 and containing 4-1BB and CD3ζ domains demonstrated in vivo CAR T-cell expansion and persistence of both effector and central memory phenotypes [35]. Anti-leukemic effects were noted in all three patients examined, with two of three patients achieving complete remission [35, 36].

In this study, we describe the identification and characterization of PF-05082566, a 4-1BB-specific agonist human IgG2 mAb for therapeutic use to enhance the immune response to tumors. PF-05082566 binds to human and cynomolgus 4-1BB with high affinity and selectivity at a site competitive with 4-1BBL. In in vitro studies, binding of PF-05082566 to primary human and cynomolgus T cells activates the NF-κB signaling pathway resulting in enhanced cytokine production.

PF-05082566 induced leukocyte proliferation in a mouse model with a systemic humanized immune system. Further, intravenous administration of PF-05082566 to

cynomolgus monkeys resulted in proliferation of CD8+ memory T cells. These observations are consistent with murine models of 4-1BB agonism as mice deficient in 4-1BBL had reduced memory responses to viral infections [37], whereas mice with transgenic expression of 4-1BBL accumulated memory T cells [38]. Mice stimulated with 4-1BB agonist mAbs showed increased proliferation of memory T cells in naive mice [38]. In xenograft models of melanoma, prostate carcinoma and colorectal carcinoma with a locally humanized immune system, PF-05082566 demonstrated single agent efficacy, suggesting that PF-05082566 represents a 4-1BB agonist mAb that may deliver meaningful benefit to cancer patients.

Although 4-1BB stimulation has demonstrated significant anti-tumor effects, there is the potential for adverse consequences of therapeutic antibody-mediated immune system modulation. Mice treated with anti-4-1BB agonist mAbs demonstrated alterations in hematopoiesis and lymphocyte trafficking as well as multifocal, polyclonal CD8 T-cell liver infiltration [17, 18]. Adverse effects following administration of 4-1BB agonist mAbs were not reported in several studies in non-human primates [39–41]. However, in phase I studies of BMS-663513, an anti-human 4-1BB antibody of human IgG4 isotype, elevation of AST and ALT was among the most frequent ≥grade 2 laboratory abnormalities [19]. A phase II study of BMS-663513 as second line monotherapy in metastatic melanoma was terminated in May 2009 due to a high incidence of grade 4 hepatitis [20]. PF-05082566 was well tolerated in monkeys following single doses of up to 10 mg/kg, and weekly doses up to 5 mg/kg. Following weekly doses of >5 mg/kg, dose-limiting toxicities were observed. A detailed description of the toxicity profile of PF-05082566 in monkeys is beyond the scope of this report and will be presented elsewhere (manuscript in preparation). This highlights the potential value of 4-1BB as an

immunomodulatory target. However, based on pre-clinical and early clinical data, it is clear that, as with many anti-cancer agents, care must be taken to optimize efficacy while maintaining a tolerable toxicity profile.

In vitro studies of PF-05082566 demonstrated a bell-shaped response curve for cytokine release. It is possible that that this is an artifact of in vitro culture system as evidence of a bell shaped response curve was not noted in vivo in the huPBL-SCID-Bg xenograft model and in cynomolgus monkeys at doses up to 10 mg/kg. Multiple doses of PF-05082566 at 100 mg/kg, were able to induce significant lymphocyte proliferation in cynomolgus monkeys although the magnitude of proliferation was lower than that noted for doses of 5 mg/kg. The reason for this relative reduction in lymphocyte proliferation in the peripheral blood compartment is unclear but may related to altered lymphocyte trafficking or toxicity noted at the highest doses in this study.

Cross-linking of PF-05082566 using either anti-human F(ab′)2 secondary mAbs or immobilization to tissue culture plastic was required for in vitro activity of PF-05082566 as minimal evidence of activation was noted when PF-05082566 was added directly to culture media. Recent studies of rodent agonistic antibodies to CD40 (TNFRSF5) in murine models have suggested that interactions with inhibitory Fcγ receptors (FcγR) are required for optimal immunostimulatory and anti-tumor activity of anti-CD40 mAbs and may be an important component of activity for agonistic mAbs specific for other TNFR family members [42, 43]. As human IgG2 and IgG4 mAbs have reduced binding capability to FcγR compared with other IgG istoypes, this is an important consideration for generating agents for therapeutic use. However, CP-870,893 a human IgG2 mAb specific for CD40, was able to activate B-cell and dendritic cell function in vitro, had anti-tumor activity in several xenograft models and demonstrated immune modulation and clinical activity in Ph1 trials [44–48]. Studies of the non-germlined parental mAb of PF-05082566 demonstrated similar activity of IgG1, IgG2, and IgG4 isotype variants in vitro and in vivo during huPBL-SCID-Bg xenograft studies (Supplemental Figure 3B and data not shown). The level of anti-tumor activity noted for these antibodies was similar to that shown for PF-05082566 in Fig. 6.

The reasons for the apparent differential requirement for inhibitory FcγR ligation for CD40 agonist mAbs are unclear. However, possibilities include differences in requirement for FcγR binding based on the specific epitope recognized by individual CD40 agonist mAbs, differential requirement for binding in rodent versus primate species, or differences in the sensitivity of model systems to detect the requirement for FcγR binding. It is also possible that this phenomenon noted for rodent CD40 agonist mAbs may

be specific for mAbs that induce immune activation through modulation of antigen-presenting cells rather than those that target T cells more directly.

Here, we have presented similar anti-tumor activity of isotype variants of 4-1BB agonist mAbs. Further, multiple human IgG4 4-1BB agonist antibodies demonstrated enhanced cellular immunity to SIV vaccines [40, 41]. In a phase I–II study of BMS-663513, biomarker studies indicated biological activity at the lowest dose tested (0.3 mg/kg) and partial response and sustained stable disease were reported at several dose levels in patients with locally advanced or metastatic solid tumors [19]. Taken together, this suggests either that FcγR binding is not critical for 4-1BB agonist mAbs or that the non-clinical models available to evaluate therapeutic agents, which are not cross-reactive with rodent species, are not sufficient to assess this interaction.

The ability of non-clinical models to accurately predict clinical efficacy has been identified as a key challenge to the development of immunomodulators for clinical use [49]. Here, we have employed several in vitro and in vivo models to assess the activity of PF-05082566. The results from these models are consistent with the mechanism of action that has been proposed for 4-1BB agonist mAbs including enhanced cytokine release and increased lymphocyte proliferation, particularly of memory T cells, and anti-tumor activity. PF-05082566 is currently being investigated for the treatment of advanced solid tumors and B-cell malignancies in phase I clinical trials (NCT01307267).

References

1. Wang C, Lin GH, McPherson AJ, Watts TH (2009) Immune regulation by 4-1BB and 4-1BBL: complexities and challenges. Immunol Rev 229(1):192–215. doi:10.1111/j.1600-065X.2009.00765.x
2. Broll K, Richter G, Pauly S, Hofstaedter F, Schwarz H (2001) CD137 expression in tumor vessel walls. High correlation with malignant tumors. Am J Clin Pathol 115(4):543–549. doi:10.1309/6U88-357U-UKJ5-YPT3
3. Seaman S, Stevens J, Yang MY, Logsdon D, Graff-Cherry C, St Croix B (2007) Genes that distinguish physiological and pathological angiogenesis. Cancer Cell 11(6):539–554. doi:10.1016/j.ccr.2007.04.017
4. Olofsson PS, Soderstrom LA, Wagsater D, Sheikine Y, Ocaya P, Lang F, Rabu C, Chen L, Rudling M, Aukrust P, Hedin U,

Paulsson-Berne G, Sirsjo A, Hansson GK (2008) CD137 is expressed in human atherosclerosis and promotes development of plaque inflammation in hypercholesterolemic mice. Circulation 117(10): 1292–1301. doi:10.1161/CIRCULATIONAHA.107.699173

5. Dawicki W, Bertram EM, Sharpe AH, Watts TH (2004) 4–1BB and OX40 act independently to facilitate robust CD8 and CD4 recall responses. J Immunol 173(10):5944–5951

6. Pollok KE, Kim YJ, Zhou Z, Hurtado J, Kim KK, Pickard RT, Kwon BS (1993) Inducible T cell antigen 4–1BB. Analysis of expression and function. J Immunol 150(3):771–781

7. Chan FK (2007) Three is better than one: pre-ligand receptor assembly in the regulation of TNF receptor signaling. Cytokine 37(2):101–107. doi:10.1016/j.cyto.2007.03.005

8. Michel J, Langstein J, Hofstadter F, Schwarz H (1998) A soluble form of CD137 (ILA/4-1BB), a member of the TNF receptor family, is released by activated lymphocytes and is detectable in sera of patients with rheumatoid arthritis. Eur J Immunol 28(1):290–295. doi:10.1002/(SICI)1521-4141(199801)28:01<290:AID-IMMU290>3.0.CO;2-S

9. Furtner M, Straub RH, Kruger S, Schwarz H (2005) Levels of soluble CD137 are enhanced in sera of leukemia and lymphoma patients and are strongly associated with chronic lymphocytic leukemia. Leukemia 19(5):883–885. doi:10.1038/sj.leu.2403675

10. Hentschel N, Krusch M, Kiener PA, Kolb HJ, Salih HR, Schmetzer HM (2006) Serum levels of sCD137 (4–1BB) ligand are prognostic factors for progression in acute myeloid leukemia but not in non-Hodgkin's lymphoma. Eur J Haematol 77(2):91–101. doi:10.1111/j.1600-0609.2006.00679.x

11. Sabbagh L, Pulle G, Liu Y, Tsitsikov EN, Watts TH (2008) ERK-dependent Bim modulation downstream of the 4-1BB-TRAF1 signaling axis is a critical mediator of CD8 T cell survival in vivo. J Immunol 180(12):8093–8101

12. Croft M (2009) The role of TNF superfamily members in T-cell function and diseases. Nat Rev Immunol 9(4):271–285. doi:10.1038/nri2526

13. Wang S, Chen L (2011) Immunobiology of cancer therapies targeting CD137 and B7-H1/PD-1 cosignal pathways. Curr Top Microbiol Immunol 344:245–267. doi:10.1007/82_2010_81

14. Lynch DH (2008) The promise of 4-1BB (CD137)-mediated immunomodulation and the immunotherapy of cancer. Immunol Rev 222:277–286. doi:10.1111/j.1600-065X.2008.00621.x

15. Palazon A, Teijeira A, Martinez-Forero I, Hervas-Stubbs S, Roncal C, Penuelas I, Dubrot J, Morales-Kastresana A, Perez-Gracia JL, Ochoa MC, Ochoa-Callejero L, Martinez A, Luque A, Dinchuk J, Rouzaut A, Jure-Kunkel M, Melero I (2011) Agonist anti-CD137 mAb act on tumor endothelial cells to enhance recruitment of activated T lymphocytes. Cancer Res 71(3):801–811. doi:10.1158/0008-5472.CAN-10-1733

16. Vinay DS, Cha K, Kwon BS (2006) Dual immunoregulatory pathways of 4-1BB signaling. J Mol Med (Berl) 84(9):726–736. doi:10.1007/s00109-006-0072-2

17. Niu L, Strahotin S, Hewes B, Zhang B, Zhang Y, Archer D, Spencer T, Dillehay D, Kwon B, Chen L, Vella AT, Mittler RS (2007) Cytokine-mediated disruption of lymphocyte trafficking, hemopoiesis, and induction of lymphopenia, anemia, and thrombocytopenia in anti-CD137-treated mice. J Immunol 178(7):4194–4213

18. Dubrot J, Palazon A, Alfaro C, Azpilikueta A, Ochoa MC, Rouzaut A, Martinez-Forero I, Teijeira A, Berraondo P, Le Bon A, Hervas-Stubbs S, Melero I (2011) Intratumoral injection of interferon-alpha and systemic delivery of agonist anti-CD137 monoclonal antibodies synergize for immunotherapy. Int J Cancer 128(1):105–118. doi:10.1002/ijc.25333

19. Sznol M, Hodi FS, Margolin K, McDermott DF, Ernestoff S, Kirkwood JM (2008) Phase I study of BMS-663513, a fully human anti-CD137 agonist monoclonal antibody, in patients with advanced cancer. J Clin Oncol 26(115S):3007

20. Ascierto PA, Simeone E, Sznol M, Fu YX, Melero I (2010) Clinical experiences with anti-CD137 and anti-PD1 therapeutic antibodies. Semin Oncol 37(5):508–516. doi:10.1053/j.seminoncol.2010.09.008

21. Chen SJ, Foster WR, Jure-Kunkel MN, Girit E, Abraham R, Hefta LJ, Gao S, Yonan CR, Lin JH, Dambach DM (2008) Cloning, expression and characterization of monkey (Macaca fascicularis) CD137. Vet Immunol Immunopathol 126(3–4): 377–381. doi:10.1016/j.vetimm.2008.07.009

22. King M, Pearson T, Shultz LD, Leif J, Bottino R, Trucco M, Atkinson MA, Wasserfall C, Herold KC, Woodland RT, Schmidt MR, Woda BA, Thompson MJ, Rossini AA, Greiner DL (2008) A new Hu-PBL model for the study of human islet alloreactivity based on NOD-scid mice bearing a targeted mutation in the IL-2 receptor gamma chain gene. Clin Immunol 126(3):303–314. doi:10.1016/j.clim.2007.11.001

23. Pitcher CJ, Hagen SI, Walker JM, Lum R, Mitchell BL, Maino VC, Axthelm MK, Picker LJ (2002) Development and homeostasis of T cell memory in rhesus macaque. J Immunol 168(1): 29–43

24. Shultz LD, Ishikawa F, Greiner DL (2007) Humanized mice in translational biomedical research. Nat Rev Immunol 7(2):118–130. doi:10.1038/nri2017

25. Iwanuma Y, Chen FA, Egilmez NK, Takita H, Bankert RB (1997) Antitumor immune response of human peripheral blood lymphocytes coengrafted with tumor into severe combined immunodeficient mice. Cancer Res 57(14):2937–2942

26. Sondak VK, Smalley KS, Kudchadkar R, Grippon S, Kirkpatrick P (2011) Ipilimumab. Nat Rev Drug Discov 10(6):411–412. doi:10.1038/nrd3463

27. Lesterhuis WJ, Haanen JB, Punt CJ (2011) Cancer immunotherapy—revisited. Nat Rev Drug Discov 10(8):591–600. doi:10.1038/nrd3500

28. Cheever MA (2008) Twelve immunotherapy drugs that could cure cancers. Immunol Rev 222:357–368. doi:10.1111/j.1600-065X.2008.00604.x

29. Schabowsky RH, Elpek KG, Madireddi S, Sharma RK, Yolcu ES, Bandura-Morgan L, Miller R, MacLeod KJ, Mittler RS, Shirwan H (2009) A novel form of 4-1BBL has better immunomodulatory activity than an agonist anti-4-1BB Ab without Ab-associated severe toxicity. Vaccine 28(2):512–522. doi:10.1016/j.vaccine.2009.09.127

30. McNamara JO, Kolonias D, Pastor F, Mittler RS, Chen L, Giangrande PH, Sullenger B, Gilboa E (2008) Multivalent 4–1BB binding aptamers costimulate CD8+ T cells and inhibit tumor growth in mice. J Clin Invest 118(1):376–386. doi:10.1172/JCI33365

31. Milone MC, Fish JD, Carpenito C, Carroll RG, Binder GK, Teachey D, Samanta M, Lakhal M, Gloss B, Danet-Desnoyers G, Campana D, Riley JL, Grupp SA, June CH (2009) Chimeric receptors containing CD137 signal transduction domains mediate enhanced survival of T cells and increased antileukemic efficacy in vivo. Mol Ther 17(8):1453–1464. doi:10.1038/mt.2009.83

32. Song DG, Ye Q, Carpenito C, Poussin M, Wang LP, Ji C, Figini M, June CH, Coukos G, Powell DJ Jr (2011) In vivo persistence, tumor localization, and antitumor activity of CAR-engineered T cells is enhanced by costimulatory signaling through CD137 (4-1BB). Cancer Res 71(13):4617–4627. doi:10.1158/0008-5472.CAN-11-0422

33. Finney HM, Akbar AN, Lawson AD (2004) Activation of resting human primary T cells with chimeric receptors: costimulation from CD28, inducible costimulator, CD134, and CD137 in series with signals from the TCR zeta chain. J Immunol 172(1):104–113

34. Sadelain M, Brentjens R, Riviere I (2009) The promise and potential pitfalls of chimeric antigen receptors. Curr Opin Immunol 21(2):215–223. doi:10.1016/j.coi.2009.02.009

35. Kalos M, Levine BL, Porter DL, Katz S, Grupp SA, Bagg A, June CH (2011) T cells with chimeric antigen receptors have potent antitumor effects and can establish memory in patients with advanced leukemia. Sci Transl Med 3(95):95ra73. doi:10.1126/scitranslmed.3002842

36. Porter DL, Levine BL, Kalos M, Bagg A, June CH (2011) Chimeric antigen receptor-modified T cells in chronic lymphoid leukemia. N Engl J Med 365(8):725–733. doi:10.1056/NEJMoa1103849

37. Tan JT, Whitmire JK, Ahmed R, Pearson TC, Larsen CP (1999) 4–1BB ligand, a member of the TNF family, is important for the generation of antiviral CD8 T cell responses. J Immunol 163(9):4859–4868

38. Zhu Y, Zhu G, Luo L, Flies AS, Chen L (2007) CD137 stimulation delivers an antigen-independent growth signal for T lymphocytes with memory phenotype. Blood 109(11):4882–4889. doi:10.1182/blood-2006-10-043463

39. Hong HJ, Lee JW, Park SS, Kang YJ, Chang SY, Kim KM, Kim JO, Murthy KK, Payne JS, Yoon SK, Park MJ, Kim IC, Kim JG, Kang CY (2000) A humanized anti-4-1BB monoclonal antibody suppresses antigen-induced humoral immune response in non-human primates. J Immunother 23(6):613–621

40. Calarota SA, Hokey DA, Dai A, Jure-Kunkel MN, Balimane P, Weiner DB (2008) Augmentation of SIV DNA vaccine-induced cellular immunity by targeting the 4-1BB costimulatory molecule. Vaccine 26(25):3121–3134. doi:10.1016/j.vaccine.2008.02.017

41. Hirao LA, Hokey DA, Morrow MP, Jure-Kunkel MN, Weiner DB (2011) Immune modulation through 4-1BB enhances SIV vaccine protection in non-human primates against SIVmac251 challenge. PLoS ONE 6(9):e24250. doi:10.1371/journal.pone.0024250

42. Li F, Ravetch JV (2011) Inhibitory Fcgamma receptor engagement drives adjuvant and anti-tumor activities of agonistic CD40 antibodies. Science 333(6045):1030–1034. doi:10.1126/science.1206954

43. White AL, Chan HT, Roghanian A, French RR, Mockridge CI, Tutt AL, Dixon SV, Ajona D, Verbeek JS, Al-Shamkhani A, Cragg MS, Beers SA, Glennie MJ (2011) Interaction with FcgammaRIIB is critical for the agonistic activity of anti-CD40 monoclonal antibody. J Immunol 187(4):1754–1763. doi:10.4049/jimmunol.1101135

44. Gladue RP, Paradis T, Cole SH, Donovan C, Nelson R, Alpert R, Gardner J, Natoli E, Elliott E, Shepard R, Bedian V (2011) The CD40 agonist antibody CP-870,893 enhances dendritic cell and B-cell activity and promotes anti-tumor efficacy in SCID-hu mice. Cancer Immunol Immunother 60(7):1009–1017. doi:10.1007/s00262-011-1014-6

45. Hunter TB, Alsarraj M, Gladue RP, Bedian V, Antonia SJ (2007) An agonist antibody specific for CD40 induces dendritic cell maturation and promotes autologous anti-tumour T-cell responses in an in vitro mixed autologous tumour cell/lymph node cell model. Scand J Immunol 65(5):479–486. doi:10.1111/j.1365-3083.2007.01927.x

46. Carpenter EL, Mick R, Ruter J, Vonderheide RH (2009) Activation of human B cells by the agonist CD40 antibody CP-870,893 and augmentation with simultaneous toll-like receptor 9 stimulation. J Transl Med 7:93. doi:10.1186/1479-5876-7-93

47. Ruter J, Antonia SJ, Burris HA, Huhn RD, Vonderheide RH (2010) Immune modulation with weekly dosing of an agonist CD40 antibody in a phase I study of patients with advanced solid tumors. Cancer Biol Ther 10(10):983–993. doi:10.4161/cbt.10.10.13251

48. Beatty GL, Chiorean EG, Fishman MP, Saboury B, Teitelbaum UR, Sun W, Huhn RD, Song W, Li D, Sharp LL, Torigian DA, O'Dwyer PJ, Vonderheide RH (2011) CD40 agonists alter tumor stroma and show efficacy against pancreatic carcinoma in mice and humans. Science 331(6024):1612–1616. doi:10.1126/science.1198443

49. Fox BA, Schendel DJ, Butterfield LH, Aamdal S, Allison JP, Ascierto PA, Atkins MB, Bartunkova J, Bergmann L, Berinstein N, Bonorino CC, Borden E, Bramson JL, Britten CM, Cao X, Carson WE, Chang AE, Characiejus D, Choudhury AR, Coukos G, de Gruijl T, Dillman RO, Dolstra H, Dranoff G, Durrant LG, Finke JH, Galon J, Gollob JA, Gouttefangeas C, Grizzi F, Guida M, Hakansson L, Hege K, Herberman RB, Hodi FS, Hoos A, Huber C, Hwu P, Imai K, Jaffee EM, Janetzki S, June CH, Kalinski P, Kaufman HL, Kawakami K, Kawakami Y, Keilholtz U, Khleif SN, Kiessling R, Kotlan B, Kroemer G, Lapointe R, Levitsky HI, Lotze MT, Maccalli C, Maio M, Marschner JP, Mastrangelo MJ, Masucci G, Melero I, Nelief C, Murphy WJ, Nelson B, Nicolini A, Nishimura MI, Odunsi K, Ohashi PS, O'Donnell-Tormey J, Old LJ, Ottensmeier C, Papamichail M, Parmiani G, Pawelec G, Proietti E, Qin S, Rees R, Ribas A, Ridolfi R, Ritter G, Rivoltini L, Romero PJ, Salem ML, Scheper RJ, Seliger B, Sharma P, Shiku H, Singh-Jasuja H, Song W, Straten PT, Tahara H, Tian Z, van Der Burg SH, von Hoegen P, Wang E, Welters MJ, Winter H, Withington T, Wolchok JD, Xiao W, Zitvogel L, Zwierzina H, Marincola FM, Gajewski TF, Wigginton JM, Disis ML (2011) Defining the critical hurdles in cancer immunotherapy. J Transl Med 9(1):214. doi:10.1186/1479-5876-9-214